PHYSICAL REVIEW D **89,** 096003 (2014)

Operator definition and derivation of collisional energy and momentum loss in relativistic plasmas

R. B. Neufeld[*]
Electro Magnetic Applications, Lakewood, Colorado 80226, USA

Ivan Vitev[†]
Los Alamos National Laboratory, Theoretical Division, MS B238, Los Alamos, New Mexico 87545, USA

Hongxi Xing[‡]
Institute of Particle Physics, Central China Normal University, Wuhan 430079, China and Los Alamos National Laboratory, Theoretical Division, MS B238, Los Alamos, New Mexico 87545, USA

(Received 27 January 2014; published 8 May 2014)

We present an operator definition of the collisional energy and momentum loss suffered by an energetic charged particle in the presence of a medium. Our approach uses the energy-momentum tensor of the medium to evaluate the energy and momentum transfer rates. We apply this formalism to an energetic lepton or quark propagating in thermal electron-positron or quark-gluon plasmas, respectively. By using two different approaches to describe the energetic charged particle, an external current approach and a diagrammatic approach, we show explicitly that the operator method reproduces the known results for collisional energy loss from the scattering rate formalism. We further use our results to evaluate the collisional energy and momentum loss for the cases of heavy quark propagation through a quark-gluon plasma and energetic muon propagation in an electron-positron plasma produced in a high-intensity laser field.

DOI: 10.1103/PhysRevD.89.096003 PACS numbers: 52.27.Ny, 12.20.-m, 12.38.Bx

I. INTRODUCTION

In recent years, the study of the properties of the medium created in high energy nucleus-nucleus collisions has attracted tremendous attention from both experiment and theory. In unraveling these medium properties, jet quenching [1], which refers to the suppression of the production rate of high transverse momentum (p_T) leading particles and jets in relativistic heavy-ion reactions relative to a naive superposition of nucleon-nucleon collisions, is thought to provide valuable information about the properties of the quark-gluon plasma (QGP) [1] and cold nuclear matter (CNM) [2,3]. This suppression has been attributed to the energy loss of high-p_T partons due to interactions between the energetic jet and the medium through elastic and inelastic scattering. There have been multiple studies of the energy loss based on perturbative QCD, where radiative energy loss [4–9] is thought to dominate the leading particle and jet attenuation and the collisional energy loss is relatively small. Experimental data on heavy meson attenuation from both RHIC [10–12] and the LHC [13,14], however, suggest that radiative energy loss alone may not be sufficient to describe the magnitude of the observed attenuation. Collisional effects, such as energy loss and hadron dissociation, may play a role in heavy flavor quenching [15–19]. The cumulative effect of collisional energy loss is also amplified in a parton shower and can be studied in jet observables [20–24], especially for large radii R [25].

The first perturbative estimate of the collisional energy loss rate dE/dx was made by Bjorken [26]. Subsequently, Braaten and Thoma (hereafter referred to as BT) performed a calculation of dE/dx where the energy loss was defined as the average over the interaction rate Γ of the energy transfer ω and divided by the velocity u of the energetic parton [27]. This is expressed in a symbolic formula as

$$\frac{dE}{dx} = \frac{1}{u}\int d\Gamma\omega, \tag{1}$$

where the energy loss can be calculated analogously to the interaction rate from either the scattering matrix element or the imaginary part of the energetic parton self-energy.

Most calculations of collisional energy loss have focused on the perspective of the energetic particle as it propagates in the medium and suffers losses through scattering. A different point of view, which we will emphasize here, is the perspective of the medium as it observes and responds to the propagating particle. This is especially

[*]bryon@ema3d.com
[†]ivitev@lanl.gov
[‡]hxing@lanl.gov

useful when we are interested in collective phenomena in electromagnetic and strongly interacting plasmas [28–30].

At a fundamental level, the properties and dynamics of a medium—including the energy transfer rate of an energetic particle into the medium—are contained in its energy-momentum tensor defined in terms of the underlying fields. Explicitly, the four-momentum loss dP^ν/dt per unit time (throughout this paper we use capital letters to denote four-momentum) can be related to the spatial integration of the individual components of the energy-momentum tensor as [31,32]

$$\frac{dP^\nu}{dt} = \int d^3x \langle \partial_\mu T^{\mu\nu}(X) \rangle_\beta. \tag{2}$$

Here, $T^{\mu\nu}$ is the medium energy-momentum tensor (EMT) and summation over repeated indices is implied. In QED and QCD, $T^{\mu\nu}$ is an operator defined in terms of quantum fields; we therefore refer to Eq. (2) as an operator definition of four-momentum loss rate. Early analysis of the medium energy-momentum tensor response to an energetic particle was based in the desire to understand the medium response in the form of shockwaves or Mach cones. The quantity $\langle \partial_\mu T^{\mu\nu}(X) \rangle_\beta$ (or source term) in Eq. (2) above not only contains information about the collisional energy loss but also acts as a seed for the fluid dynamic response of the medium to a fast particle. $\langle \cdots \rangle_\beta$ denotes the thermal expectation value of the operator in the medium.

Many significant attempts have been made to understand the energy-momentum deposition (i.e. source term) profile in QCD and related observables [33–45]. However, there exists no rigorous theoretical definition or first principles calculation on how the lost energy is deposited along the way as the jet propagates through the medium. In the weakly coupling region, all of the calculations are based on the result from the perspective of the fast parton, which in principle should be calculated from the medium's point of view as it observes and responds to the fast parton. In the strongly coupled limit, the AdS/CFT correspondence has been used to evaluate the stress tensor within the context of linearized gravity [46–48]. Recently, in the weakly interacting limit, attempts have been made to calculate from first principles the energy deposition of a fast parton and a parton shower traversing the QGP in terms of the medium energy-momentum tensor $T^{\mu\nu}$ [49,50] to leading logarithmic accuracy. These works considered only the soft momentum transfer mode and the results depend logarithmically on the cutoff scales, which were introduced to regularize the infrared and ultraviolet divergences. Furthermore, the incident particle was modeled as a classical current. To eliminate the ambiguities due to the choice of scales, in this paper we perform a complete calculation by including both the soft and hard modes. We also show explicitly that using two different approaches to describe the energetic charged particle, an external current approach and a diagrammatic approach, yields the same results for dP^ν/dt.

In this paper, with the help of Feynman rules that have been derived from the operator definition of the EMT [49], we will compute the collisional energy transfer rate including both soft and hard contributions. Our analysis shows that the energy-momentum tensor provides a natural and powerful way to approach collisional energy and momentum deposition, and can be extended to many systems of physical interest. The outline of the paper is as follows: we present the theoretical formalism for the evaluation of the medium response in Sec. II. In Sec. III we apply our formalism to an energetic lepton propagating in a thermal electron-positron plasma (EPP) by using the external current approach, and to energetic quarks traveling in a quark-gluon plasma using a much more general diagrammatic approach. We show that these two approaches reproduce the result for collisional energy loss from the scattering rate formalism. We further show in Sec. IV the numerical result for the collisional energy-momentum transfer rate in the case of experimentally relevant QED and QCD plasmas. Our summary is given in Sec. V.

II. FORMALISM

In this section we present the formalism used in the paper. We focus on the medium EMT $T^{\mu\nu}$ in the presence of a fast parton created in the distant past. We are particularly interested in the divergence of the EMT, or the source term J^ν. The source term is useful because it provides a way to obtain the energy and momentum loss from the medium's point of view [as shown in Eq. (2)] and also drives the bulk evolution of the medium. We present our results in a general integral form, which we will use in later sections to extract a specific quantity, namely the collisional energy and momentum loss of an energetic lepton or quark.

At a fundamental level, the properties and dynamics of a medium are contained in its energy-momentum tensor defined in terms of the underlying fields. We begin this section by introducing this important quantity with an eye on how we will set up the problem of evaluating it in the presence of a fast lepton. We consider a medium of massless electrons and positrons with conventional field notation: fermion fields are denoted by ψ and photon fields by A. The QED EMT is given by [51]

$$T^{\mu\nu} = \frac{i}{4}\bar{\psi}(\gamma^\mu \overleftrightarrow{D}^\nu + \gamma^\nu \overleftrightarrow{D}^\mu)\psi - g^{\mu\nu}\mathcal{L}_F, \tag{3}$$

where

$$\mathcal{L}_F = \frac{i}{2}\bar{\psi}\overleftrightarrow{\not{D}}\psi, \qquad D^\mu = \partial^\mu - ieA^\mu \tag{4}$$

and

$$\bar{\psi}\gamma^{\mu}\overleftrightarrow{D}^{\nu}\psi = \bar{\psi}\gamma^{\mu}\vec{D}^{\nu}\psi - \bar{\psi}\gamma^{\mu}\overleftarrow{D}^{*\nu}\psi. \tag{5}$$

In the above equations, e is the electromagnetic coupling parameter and conventional slashed notation is used, $A = \gamma_{\mu}A^{\mu}$, etc. A summation over spin is implied in the EMT.

In principle, any quantity relating to the energy and momentum of a medium can be extracted from the EMT. For example, one can use the EMT in thermal field theory to obtain perturbative corrections to the pressure or energy density of an ideal gas. Furthermore, one does not need a system in equilibrium to use the EMT. Any distribution function, whether or not it is thermal, can be used with the EMT to extract quantities of interest. The utility and breadth of applications of the EMT make it a powerful analytical tool to investigate medium properties, and provide one possible approach to bridge the short and long distance dynamics of a medium.

In order to calculate the medium response far from the fast parton, one can consider two possibilities in terms of EMT: (a) calculating individual components of the EMT directly within perturbation theory to obtain information about the medium response; (b) calculating the source term for the EMT within perturbation theory and use an effective theory to propagate the resulting disturbance to regions far from the fast parton. In some sense, the two approaches are related since both of them arise from the EMT. However, there is an essential difference between these two: the additional derivatives in the source term serve to add momentum weighting, this additional weighting changes the infrared behavior completely and makes the final result infrared safe. Therefore, we apply approach (b) in this paper to consider the problem of collisional energy and momentum loss in a thermal medium, or medium response, so that we can get a physical result that is independent of any cutoff scales. This application allows us to obtain analytical results that compare directly to previous results obtained using scattering rates. The rate of energy and momentum being transferred to a medium is related to the EMT through the equations [31,32]

$$\frac{dE}{dt} = \int d^3x \langle \partial_{\mu} T^{\mu 0}(X) \rangle_{\beta},$$
$$\frac{dp^i}{dt} = \int d^3x \langle \partial_{\mu} T^{\mu i}(X) \rangle_{\beta}. \tag{6}$$

In an isolated medium, Eq. (6) of course evaluates to zero because of energy-momentum conservation. However, when a fast projectile is being pushed through the surrounding medium, which can be represented by some external current, it must be transferring energy and momentum to the surrounding medium, meaning that the EMT is not conserved for each of the two components of the system—the medium and the projectile. Assuming we have some way to couple an external source of energy to the medium, the evaluation of the energy transfer rate can be performed using standard techniques of thermal field theory. In the rest of this section we will present the basic details of such an evaluation and present a formula that can be used for the calculation of energy-momentum transfer rates to a medium for a wide variety of problems. We will also omit the explicit thermal expectation value notation for the rest of the paper.

We will borrow some of the results presented in [49], where the EMT source term was calculated for a medium in the presence of a classical charge in the hard thermal loop (HTL) approximation. In the HTL limit the fields generated by the external current are soft compared to the medium temperature. Explicitly, the fermion propagator is expanded in the limit where the momentum of the exchanged gluon is much smaller than the one of the medium parton.

Building upon the analysis presented in the previous work, the presentation here will be extended to a much more general case by including both the hard and soft contributions. The technique of introducing an arbitrary momentum scale q^* to separate the hard and soft regions of the momentum transfer was developed in [27]. The contribution from hard momentum transfers is computed by using the tree-level propagator for the exchanged gluon, while the contribution from the soft region is computed using an effective gluon propagator. The dependence on the arbitrary scale q^* cancels upon adding the hard and soft contributions.

The lowest order Feynman diagrams for energy transfer into an electron-positron plasma is shown in Fig. 1. We do not have to consider yet what the external photons connect to, only that they will represent a two-photon exchange with the medium. The next section will provide a specific application toward collisional energy and momentum loss, but in this section the source of energy remains general. The lowest order diagrams for energy-momentum exchange require two-photon exchange that can be easily verified using Furry's theorem. The same is true for QCD. Since we are focused on the energy-momentum transfer rate in this paper, the diagrams of Fig. 1 should be evaluated using real time thermal field theory, where the diagram in Fig. 1(a) comes from the bare part of the EMT (the pieces with no

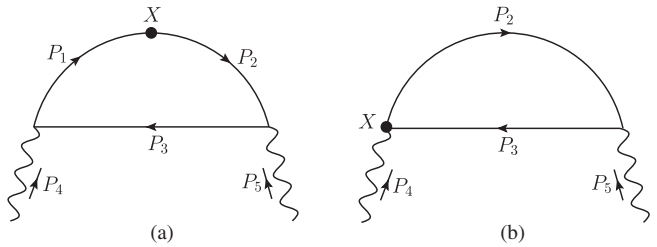

FIG. 1. Feynman diagrams contributing to $\langle \partial_{\mu} T^{\mu\nu}(x) \rangle$ in the presence of a source interaction term, $A^a_{\mu} j^{\mu}_a$. The diagram in (a) can be traced back to terms in the energy-momentum tensor [see Eq. (3)] which go as $\bar{\psi}\gamma\partial\psi$, whereas the diagram in (b) originates from terms that go as $g\bar{\psi}\gamma A\psi$.

coupling constant), and Fig. 1(b) arises from the interacting part of the EMT. The interested reader can easily verify this by noting that the bare part of the EMT contains two fields each at position X, while the interacting part contains three fields at X.

The diagrams of Fig. 1 can be evaluated using standard Feynman rules (for instance Das [52]). However, we must also consider the effect of the derivative structure from taking the divergence of the EMT. The derivatives serve to add momentum weighting to what the diagrams by themselves would yield. Specifically, we are interested in evaluating the unique momentum contributions from the term $\partial_\mu T^{\mu\nu}(x)$ in Eq. (6). Using the momentum convention shown in Fig. 1(a), we find that taking the divergence of the EMT yields a momentum weighting of

$$\frac{ie^{-iX\cdot(P_1-P_2)}}{4}\times[(P_2^2-P_1^2)\gamma^\nu+P_1^\nu(3P_2+P_1)-P_2^\nu(3P_1+P_2)]. \tag{7}$$

The exponential term arises since the EMT is evaluated in position space.

For the diagram in Fig. 1(b) we choose the convention that the photon momentum flows into the interaction position X. Therefore, the EMT contribution is

$$-iee^{-iX\cdot(P_4+P_3-P_2)}(P_4+P_3-P_2)_\mu \times\frac{(\gamma^\nu g^{\mu\sigma}+\gamma^\mu g^{\nu\sigma}-2g^{\mu\nu}\gamma^\sigma)}{2}. \tag{8}$$

Note that Eqs. (7) and (8) are only the contribution from taking the divergence of the EMT in the diagrams of Fig. 1. It is still necessary to evaluate the diagrams in a conventional manner to get the rest of the contribution. The full result for Fig. 1 is obtained using Feynman rules at finite temperature, and we will go through a few of the steps. Starting with Fig. 1(a) and using the results from Eq. (7) we have

$$\begin{aligned}\partial_\mu T_0^{\mu\nu}(X)=&-\frac{e^2}{4}\int\frac{d^4P_i}{(2\pi)^{12}}e^{-iX\cdot(P_1-P_2)}\mathrm{Tr}[((P_2^2-P_1^2)\gamma^\nu+3P_2P_1^\nu+P_1P_1^\nu-P_2P_2^\nu-3P_1P_2^\nu)P_1\gamma^\sigma P_3\gamma^\omega P_2]\\&\times[(T(P_3)G_R(P_1)+T(P_1)G_A(P_3))G_A(P_2)+T(P_2)G_R(P_3)G_R(P_1)]\times D_{\sigma\tau}(P_4)D_{\omega\lambda}(P_5)\delta^4(P_2+P_5-P_3)\\&\times\delta^4(P_1-P_4-P_3)\otimes F^{\tau\lambda}(P_4,P_5),\end{aligned} \tag{9}$$

where the notation $T_0^{\mu\nu}(X)$ means this is the contribution from the bare (or without coupling constant) part of the EMT. A few comments are in order regarding Eq. (9). First, the notation $\int d^4P_i$ means that all momenta are integrated over $\int d^4P_i=\int d^4P_1d^4P_2d^4P_3d^4P_4d^4P_5$. $D_{\sigma\tau}(P)$ is the propagator for the exchanged photon. In the limit of a hard momentum exchange $D_{\sigma\tau}(P)=(-g_{\sigma\tau})G_R(P)$; however in the soft region one must use an HTL resummed propagator for the photon exchange. More will be said on this below. The Green's function notation is

$$G_{R/A}(P)=\frac{1}{P^2\pm i\epsilon P^0} \tag{10}$$

and $T(P)$ is the medium's particle distribution function. For a thermal system of massless fermions, we have

$$T(P)=2\pi i n_F(|P^0|)\delta(P^2). \tag{11}$$

However, as pointed out above, there is no reason one has to use a thermal medium. Finally, the notation $\otimes F_{\tau\lambda}(P_4,P_5)$ simply indicates that the expression above contains explicitly only the contribution from the diagrams related to the EMT. One must attach the photons in Fig. 1 to some external source of energy-momentum to obtain a nonzero result.

We can perform the same analysis on the diagram in Fig. 1(b):

$$\begin{aligned}\partial_\mu T_I^{\mu\nu}(X)=&-\frac{e^2}{2}\int\frac{d^4P_i}{(2\pi)^{12}}e^{-iX\cdot(P_4+P_5)}\mathrm{Tr}[(\gamma^\nu g^{\mu\sigma}+\gamma^\mu g^{\nu\sigma}-2g^{\mu\nu}\gamma^\sigma)P_2\gamma^\omega P_3](P_4+P_3-P_2)_\mu\\&\times D_{\sigma\tau}(P_4)D_{\omega\lambda}(P_5)[T(P_2)G_R(P_3)+T(P_3)G_A(P_2)]\delta^4(P_2+P_5-P_3)\otimes F^{\tau\lambda}(P_4,P_5),\end{aligned} \tag{12}$$

where the notation $T_I^{\mu\nu}(X)$ means this is the contribution from the interacting (with coupling constant) part of the EMT.

What remains to be done is to combine and simplify Eqs. (9) and (12). Since we are specifying a thermal medium, we have used the relation that $P^2T(P)=0$. We have also made use of simplifications such as $P^2G_R(P)=1$ and enforced the δ functions' constraints. The final result is

$$\partial_\mu T^{\mu\nu}(X) = 8e^2 \int \frac{d^4P_i}{(2\pi)^{12}} e^{-iX\cdot(P_4+P_5)} T(P_3) D_{\sigma\tau}(P_4) D_{\omega\lambda}(P_5) G_A(P_3 - P_4) \times [2(P_3{}^\sigma P_3{}^\omega - P_3{}^\sigma P_4{}^\omega)P_5^\nu + g^{\sigma\omega} P_3 \cdot P_4 P_5^\nu - g^{\nu\sigma} P_3{}^\omega (2P_3 \cdot P_5 - P_4 \cdot P_5)] \otimes F^{\tau\lambda}(P_4, P_5). \quad (13)$$

To obtain the energy transfer rate will require an integration over all space, as indicated in Eq. (6). Equation (13) contains a fairly general expression for the energy-momentum transfer rate to an electromagnetic plasma. It was obtained from the divergence of the EMT without specifying the source of energy and momentum, except that it be coupled via two-photon exchange. However, to obtain a closed-form of the energy transfer rate we must specify $F^{\tau\lambda}(P_4, P_5)$ in Eq. (13). This will be done for the case of collisional energy loss in the next section.

III. DETAILS OF THE CALCULATION AND ANALYTIC RESULTS

As discussed throughout the paper, our goal is to evaluate the energy-momentum transfer rate, or collisional energy and momentum loss, of an energetic particle propagating through an EPP or a QGP. One possibility is to add an interaction term to the Lagrangian of the form $\mathcal{L} \to \mathcal{L} - A_\mu j^\mu$, which was presented in Ref. [49]. Here, j^μ is a classical charged current of the form $j^\mu = eU^\mu \delta(\mathbf{x} - \mathbf{u}t)$, $U^\mu = (1, \mathbf{u})$, which represents the propagating particle. We will apply this external current approach in Sec. III A. The more general approach, which will be used in Sec. III B, is to treat the energetic quark as a field, rather than a classical current. In this diagrammatic approach the field interacts with the medium through a two-gluon exchange.

A. Collisional energy loss in a QED plasma

1. External current approach

Studies of parton energy loss in the QGP are of great phenomenological interest to heavy-ion physics. It is, however, also instructive to discuss the problem of energy loss in QED. In this case, it is natural to consider an asymptotic particle traveling through a domain containing a relativistic electron-positron plasma. Following the approach developed in [49], we model the asymptotically fast lepton by an external current $j^\mu(X)$, which in turn can be expressed in momentum space as

$$j^\mu(K) = -2\pi i e U^\mu \delta(K \cdot U). \quad (14)$$

Here, K is the four-momentum exchanged with the medium, and U is the four-velocity of the propagating fast lepton.

In Fig. 2 we focus on the contribution from $F^{\tau\lambda}(P_4, P_5)$ to Eq. (13). The upper loop, which represents the EMT contribution, is shown for completeness and has been addressed in the previous section. All that is left to do is to use Feynman rules to evaluate the contribution from the fast lepton to the energy transfer rate. We find it contributes

$$F^{\tau\lambda}(P_4, P_5) = -(2\pi)^2 e^2 U^\tau U^\lambda \delta(P_4 \cdot U)\delta(P_5 \cdot U). \quad (15)$$

Combining Eq. (15) with Eq. (13) gives

$$\partial_\mu T^{\mu\nu}(X) = -8e^4 \int \frac{d^4P_i}{(2\pi)^{10}} e^{-iX\cdot(P_4+P_5)} T(P_3) D_{\sigma\tau}(P_4) \times D_{\omega\lambda}(P_5) G_A(P_3 - P_4) U^\tau U^\lambda \delta(P_4 \cdot U)\delta(P_5 \cdot U) \times [2(P_3{}^\sigma P_3{}^\omega - P_3{}^\sigma P_4{}^\omega)P_5^\nu + g^{\sigma\omega} P_3 \cdot P_4 P_5^\nu - g^{\nu\sigma} P_3{}^\omega (2P_3 \cdot P_5 - P_4 \cdot P_5)]. \quad (16)$$

The result of Eq. (16) can then be inserted in Eq. (6) to obtain the collisional energy-momentum loss. In the next subsection we will evaluate the collisional energy loss and compare our results to the ones obtained using conventional scattering methods.

Before we undertake the evaluation of Eq. (16), a few words on soft and hard contributions at finite temperature are in order. Calculations at finite temperature involving soft excitations have been known for some time to require resummation techniques to obtain gauge-invariant results [53]. On the other hand, calculations involving hard excitations do not require resummation techniques and one can apply bare perturbation theory. Soft is here formally defined as a quantity of order eT and hard is a quantity of order T or larger, where T is the temperature and e the coupling constant with $e \ll 1$. The contributions from the hard and soft excitations should be matched

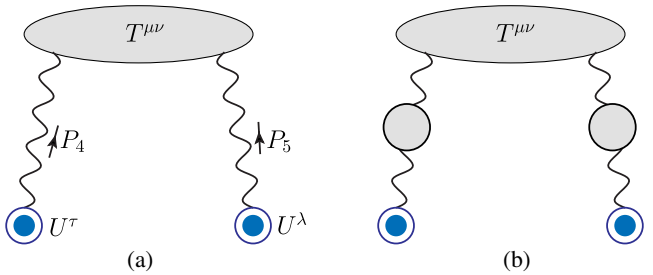

FIG. 2 (color online). Feynman diagrams for the source term in QED in the presence of the external current $J^\tau \sim U^\tau$, which is represented by the blue circle. The upper gray loop represents the EMT contribution, as shown in Fig. 1. Diagram (a) is the tree-level diagram, which contributes to the hard region. Diagram (b) contributes to the soft region and the hard thermal loop resummed photon propagator is represented by a gray blob.

consistently. A general method for carrying out the matching at finite temperature is to separate the soft and hard regimes by a separation parameter $eT \ll q^* \ll T$ [54], and then use whatever technique is most efficient in each regime separately. The final result is obtained by combining the two separate regimes into one complete calculation. The final result is independent of q^* and the result of each regime is independently gauge invariant.

We will employ this type of separation in our calculation, and verify explicitly that the final result is independent of the details of the separation. In practice, this means that the photon propagators of Eq. (10) must include the HTL resummation when evaluating the soft contribution. For the hard contribution, no such resummation is necessary.

2. Hard contribution

Starting with the expression for collisional energy loss in Eqs. (16) and (6), the contribution from the hard momentum exchange region can be cast into

$$\left.\frac{dE}{dt}\right|_{\text{hard}} = 8e^4 \int \frac{d^4P_3 d^3p_4}{(2\pi)^7} T_F(P_3) G_A(P_3 - P_4)[G_R(P_4)]^2 \times \mathbf{p}_4 \cdot \mathbf{u}[P_3 \cdot P_4 U^2 + 2(P_3 \cdot U)^2], \quad (17)$$

where we have eliminated the terms associated with $P_4^2 - 2P_3 \cdot P_4$ because these terms cancel with $G_A(P_3 - P_4)$ and the resulting P_3 integration vanishes by symmetry. In Eq. (17), P_3^0 can be integrated out by taking advantage of the δ function in T_F; then the hard contribution reduces to

$$\left.\frac{dE}{dt}\right|_{\text{hard}} = -4e^4 \int \frac{d^3p_3 d^3p_4}{(2\pi)^5 p_3} n_F(p_3)[G_R(P_4)]^2 \mathbf{p}_4 \cdot \mathbf{u} \times [2(P_3 \cdot U)^2 + U^2 P_3 \cdot P_4] \times \delta(P_4^2 - 2P_3 \cdot P_4)\text{sgn}(p_3 - \mathbf{p}_4 \cdot \mathbf{u}). \quad (18)$$

In order to simplify the expression further, it is convenient to make use of the fact that in a static medium (we can always work in its local rest frame) the collisional energy loss does not depend on the direction of $\mathbf{u}$. We can, therefore, specify a coordinate system with $\mathbf{u}$ in the $\mathbf{z}$ direction and evaluate the angular integrals in $\int d^3p_3$ and $\int d^3p_4$. On the other hand, the kinematics of the interaction between the fast lepton and the medium constrain the integration limit of p_4 and ν as follows:

$$p_4 < \frac{2p_3}{1+u\nu}, \qquad \nu < \frac{2p_3 - p_4}{p_4 u}, \quad (19)$$

where $\nu = \mathbf{u} \cdot \hat{\mathbf{p}}_4$ denotes the angle between the incident fast lepton and the exchanged photon. The kinematics limits will make $\text{sgn}(p_3 - \mathbf{p}_4 \cdot \mathbf{u})$ always positive. The collisional energy loss for the hard momentum exchange reduces to

$$\left.\frac{dE}{dt}\right|_{\text{hard}} = -e^4 \int \frac{dp_3}{(2\pi)^3} \left[\int_{q^*}^{\frac{2p_3}{1+u}} \frac{dp_4}{p_4^2} \int_{-1}^{1} d\nu + \int_{\frac{2p_3}{1+u}}^{\frac{2p_3}{1-u}} \frac{dp_4}{p_4^2} \int_{-1}^{\frac{2p_3-p_4}{p_4 u}} d\nu\right] \frac{n_F(p_3)}{(1-u^2\nu^2)^2} \times [2p_3^2(2 - 4u\nu\omega + u^2(1-\omega^2) + u^2\nu^2(3\omega^2 - 1)) - (1-u^2)p_4^2(1-u^2\nu^2)]u\nu, \quad (20)$$

where

$$\omega = \frac{p_4(1-u^2\nu^2) + 2p_3 u\nu}{2p_3}. \quad (21)$$

The maximum momentum transfer, providing the upper limit for the integration in the above equation, has been determined from the kinematics of the scattering (for discussion of kinematic limits effects see [55]).

We have enforced a lower limit for the $\int dp_4$ integration to regularize the infrared divergence, so that the remaining integrals can be evaluated analytically. Therefore, the final result of the hard contribution is free of infrared divergences. However, it depends on this cutoff scale q^* and the dependence is included in the leading logarithmic term

$$\left.\frac{dE}{dt}\right|_{\text{hard}} = \frac{e^4 T^2}{24\pi}\left[1 - \frac{1-u^2}{u}\tanh^{-1}[u]\right] \times \left(\ln\frac{T}{q^*} + \ln\frac{1}{\sqrt{1-u^2}} + C_h(u)\right), \quad (22)$$

where $C_h(u)$ is the constant term. As we can see from the above result, the logarithmic infrared divergences in the tree-level diagrams manifest themselves as logarithms of q^*. This behavior arises from long range interactions mediated by the photon. In principle, these long range interactions should be screened in the medium; therefore, one needs to resum the hard thermal loop corrections which take into account the screening.

3. Soft contribution

The soft contribution to collisional energy loss has been calculated in imaginary time formalism in terms of the imaginary part of the self-energy of the projectile lepton. Here, we perform the calculation in real time formalism for thermal field theory in terms of the energy-momentum tensor. In the region of phase space where the exchanged photon is soft, hard thermal loop corrections to the photon propagator must be resummed; the net effect is to replace the bare photon

propagator as $D^{\mu\nu}(Q)$. In the Coulomb gauge it is given by

$$D^{\mu\nu}(Q) = -P_L^{\mu\nu}\Delta_L(q_0,q) - P_T^{\mu\nu}\Delta_T(q_0,q), \quad (23)$$

where the longitudinal projector $P_L^{\mu\nu} = \delta^{\mu 0}\delta^{\nu 0}$, and the transverse projector $P_T^{00} = 0$, $P_T^{ij} = \delta^{ij} - \hat{q}^i\hat{q}^j$. The effective longitudinal and transverse propagators are

$$\Delta_L^{-1}(q_0,q) = q^2 - \frac{3}{2}m_\gamma^2\left[\frac{q_0}{q}\ln\frac{q_0+q}{q_0-q} - 2\right],$$
$$\Delta_T^{-1}(q_0,q) = q_0^2 - q^2 + \frac{3}{2}m_\gamma^2\left[\frac{q_0(q_0^2-q^2)}{2q^3}\ln\frac{q_0+q}{q_0-q} - \frac{q_0^2}{q^2}\right], \quad (24)$$

where $m_\gamma = eT/3$ is the photon screening mass. Inserting this effective photon propagator into the expression for collisional energy loss, the nonzero contribution from the Dirac traces is

$$\left.\frac{dE}{dt}\right|_{\rm soft} = -8e^4\int\frac{d^4P_3d^3p_4}{(2\pi)^7}T_F(P_3)G_A(P_3-P_4) \times [|\Delta_L(P_4)|^2H_{LL} + 2{\rm Re}(\Delta_L(P_4)\Delta_T^*(P_4))H_{LT} + |\Delta_T(P_4)|^2H_{TT}]. \quad (25)$$

Here, H_{LL} and H_{TT} arise from the longitudinal and transverse components of the effective photon propagator, respectively, and H_{LT} is the interference between them:

$$H_{LL} = \mathbf{p}_4\cdot\mathbf{u}[P_3\cdot P_4 - 2p_3^0\mathbf{p}_4\cdot\mathbf{u} + 2(p_3^0)^2],$$
$$H_{LT} = \mathbf{p}_4\cdot\mathbf{u}[\hat{\mathbf{p}}_4\cdot\mathbf{u}(\mathbf{p}_3\cdot\hat{\mathbf{p}}_4\mathbf{p}_4\cdot\mathbf{u} - 2p_3^0\mathbf{p}_3\cdot\hat{\mathbf{p}}_4) - \mathbf{p}_4\cdot\mathbf{u}(\mathbf{p}_3\cdot\mathbf{u} + p_3^0) + 2p_3^0\mathbf{p}_3\cdot\mathbf{u}],$$
$$H_{TT} = \mathbf{p}_4\cdot\mathbf{u}[-2(\mathbf{p}_3\cdot\mathbf{u} - \mathbf{p}_3\cdot\hat{\mathbf{p}}_4\hat{\mathbf{p}}_4\cdot\mathbf{u})^2 + P_3\cdot P_4((\hat{\mathbf{p}}_4\cdot\mathbf{u})^2 - u^2)]. \quad (26)$$

We further integrate over p_3^0 by taking advantage of the delta function $\delta(P_3^2)$ in $T_F(P_3)$. In the soft region, where $p_4^0 \ll p_3$ and $p_4 \ll p_3$, the δ function $\delta(P_4^2 - 2P_3\cdot P_4)$, which arises from the imaginary part of $G_A(P_3-P_4)$, reduces to $\delta(\omega - \hat{\mathbf{p}}_4\cdot\mathbf{u})$, with $\omega = \hat{\mathbf{p}}_3\cdot\hat{\mathbf{p}}_4$. Therefore, the soft contribution to the energy loss reduces to

$$\left.\frac{dE}{dt}\right|_{\rm soft} = e^4\int\frac{d^3p_3d^3p_4}{(2\pi)^5p_3^2p_4}n_F(p_3) \times\delta(\omega-\hat{\mathbf{p}}_4\cdot\mathbf{u}){\rm sgn}(p_3-\mathbf{p}_4\cdot\mathbf{u}) \times[|\Delta_L(P_4)|^2H_{LL} + 2{\rm Re}(\Delta_L(P_4)\Delta_T^*(P_4))H_{LT} + |\Delta_T(P_4)|^2H_{TT}]. \quad (27)$$

In a statical medium, the collisional energy loss does not depend on the direction of $\mathbf{u}$. Therefore, dE/dt can be further simplified by averaging the integrand over the direction of $\mathbf{u}$ by using the following formulas:

$$\int\frac{d\Omega}{4\pi}\delta(\omega-\hat{\mathbf{p}}_4\cdot\mathbf{u}) = \frac{1}{2u}\theta(u^2-\omega^2),$$
$$\int\frac{d\Omega}{4\pi}\delta(\omega-\hat{\mathbf{p}}_4\cdot\mathbf{u})u^i = \frac{1}{2u}\theta(u^2-\omega^2)\omega\hat{\mathbf{p}}_4^i,$$
$$\int\frac{d\Omega}{4\pi}\delta(\omega-\hat{\mathbf{p}}_4\cdot\mathbf{u})u^iu^j = \frac{1}{2u}\theta(u^2-\omega^2)\frac{1}{2}[(u^2-\omega^2) \times\delta^{ij} + (3\omega^2-u^2)\hat{\mathbf{p}}_4^i\hat{\mathbf{p}}_4^j], \quad (28)$$

where $\int d\Omega$ represents integration over the angles of $\mathbf{u}$. Because of the θ function in the above angular integration of $\mathbf{u}$, the integration limits of p_4^0 are constrained to the spacelike interval $-up_4 < p_4^0 < up_4$; these constraints make ${\rm sgn}(p_3 - \mathbf{p}_4\cdot\mathbf{u})$ positive. On the other hand, we enforce an arbitrary upper limit cutoff q^* (but the same as that in the hard region) to the integration of $\int dp_4$; thus the soft contribution to energy loss reduces to

$$\left.\frac{dE}{dt}\right|_{\rm soft} = \frac{2}{u}\frac{e^4}{(2\pi)^3}\int dp_3p_3n_F(p_3)\int_0^{q^*}dp_4\int_{-up_4}^{up_4}dp_4^0(p_4^0)^2 \times\left[|\Delta_L(P_4)|^2 + \frac{1}{2}\left(1-\left(\frac{p_4^0}{p_4^2}\right)^2\right) \times\left(u^2-\left(\frac{p_4^0}{p_4^2}\right)^2\right)|\Delta_T(P_4)|^2\right]. \quad (29)$$

This result matches that by BT [27], and it can be further simplified by performing the remaining integrations of $\int dp_4$ and $\int dp_4^0$; the integrals can be evaluated analytically up to the leading logarithmic term,

$$\left.\frac{dE}{dt}\right|_{\rm soft} = \frac{e^4T^2}{24\pi}\left[1-\frac{1-u^2}{u}\tanh^{-1}[u]\right]\left(\ln\frac{q^*}{3m_\gamma} + C_s(u)\right), \quad (30)$$

where the constant term $C_s(u)$ can be evaluated numerically. The expression for it can be found in Eq. (41) of [27]. Notice that the dependence on the arbitrary scale q^* only exist in the leading logarithmic term. As anticipated, it exactly cancels that from the hard contribution in Eq. (22).

4. Complete result

The complete result for the collisional energy loss to leading order is the sum of the hard contribution in Eq. (22) and soft contribution in Eq. (30):

$$\frac{dE}{dt} = \frac{e^4 T^2}{24\pi}\left[1 - \frac{1-u^2}{u}\tanh^{-1}[u]\right] \times \left(\ln\frac{T}{3m_\gamma} + \ln\frac{1}{\sqrt{1-u^2}} + C(u)\right), \quad (31)$$

where the constant term $C(u) = C_h(u) + C_s(u)$. As we can see from the final result, the dependence on the arbitrary scale q^* that separates the hard and soft regions of the momentum transfer p_4 cancels, leaving a logarithm of $1/e$. Importantly, by comparing our result for the collisional energy loss to the one in Ref. [27], we see that the collisional energy losses from the EMT formalism and the scattering rate formalism are exactly the same for both the leading logarithmic term and the constant term. There is an overall minus sign difference, which indicates that the energy lost by the charged fermion is transferred to the medium completely.

Similarly, one can obtain the collisional momentum loss by substituting the source term from Eq. (6) into the definition of momentum loss in Eq. (16). We found that the collisional momentum loss is closely related to energy loss

$$\frac{dp^z}{dt} = \frac{1}{u}\frac{dE}{dt}; \quad (32)$$

here we have chosen the fast lepton to propagate in the z direction. In this case, the linear momenta in the x and y directions are conserved: $dp^x/dt = dp^y/dt = 0$.

In the ultrarelativistic limit $u \to 1$, Eq. (17) for the hard contribution to energy loss breaks down since the upper limit of the momentum transfer p_4 goes to infinity. In this case, one must enforce an upper limit q_m on the momentum transfer, use it in the other part of the calculation, and take the $u \to 1$ limit. Thus, the hard contribution can be written as

$$\left.\frac{dE}{dt}\right|_{\text{hard}}^{u\to 1} = \frac{e^4 T^2}{48\pi}\left[\ln\frac{q_m T}{(q^*)^2} + \frac{8}{3} - 12\ln(A) + \ln(4\pi)\right], \quad (33)$$

where A is Glaisher's constant with numerical value $A \simeq 1.282$. The soft contribution is simply the $u \to 1$ limit of Eq. (30), which is the same as that from the scattering rate [Eq. (62) in Ref. [27]]:

$$\left.\frac{dE}{dt}\right|_{\text{soft}}^{u\to 1} = \frac{e^4 T^2}{24\pi}\left[\ln\frac{q^*}{3m_\gamma} + 0.256\right]. \quad (34)$$

Adding the hard and soft contributions together, the dependence on the separation scale q^* cancels and the total collisional energy loss rate is

$$\left.\frac{dE}{dt}\right|^{u\to 1} = \frac{e^4 T^2}{48\pi}\left[\ln\frac{E}{e^2 T} + 2.725\right]. \quad (35)$$

For the sake of completeness, we mention that the operator (source term) definition of collisional energy loss can also be implemented using kinetic theory, but only for the soft contribution. Hence, to obtain a full result (both soft and hard) the field theory approach is necessary. The kinetic theory implementation to extract the EMT coupled to a source of energy can be found in Ref. [56], where a QCD plasma was considered. It uses a Vlasov equation in which the external force is generated by a classical charged current. The EMT is obtained by taking momentum moments of the resulting Vlasov equation and one can obtain the energy transfer rate in the same manner as suggested in Eq. (6) of this paper. The kinetic theory approach is more straightforward, but also less versatile. It cannot be used to extract the hard contribution, and it is unclear how one can apply a more general external sources of energy, such as a parton shower.

B. Collisional energy loss in the QGP

The quark energy loss in a QGP is readily derived from the QED result; the contribution from the quark component of the medium is obtained by multiplying Eq. (31) by the number of active quark flavors N_F and by the color factor $C_2 = (N_c^2 - 1)/(4N_c)$. Introducing the QCD coupling by $e^2 \to g^2$, we obtain the quark collisional energy loss in QGP

$$\frac{dE}{dt} = \frac{g^4 T^2 C_2 N_F}{24\pi}\left[1 - \frac{1-u^2}{u}\tanh^{-1}[u]\right] \times \left(\ln\frac{T}{3m_g} + \ln\frac{1}{\sqrt{1-u^2}} + \mathcal{O}(1)\right), \quad (36)$$

where $m_g = \frac{gT}{\sqrt{3}}(1 + N_F/6)^{1/2}$ is the gluon Debye mass in the QGP. Let us clarify what the above result means. For direct comparison to the electron-positron plasmas we have shown only the quark-quark scattering channel. The HTL propagator, however, does include gluon fluctuations as can be seen from the expression for m_g. Note that if we include quark-gluon scattering the leading logarithmic result is obtained as $N_F/6 \to 1 + N_F/6$. Here, the t-channel scattering dominates.

Besides the external current approach that we have presented in the last subsection, the more general approach, which we adopt in this subsection, is to treat the energetic particle as a field rather than a classical current. This field then interacts with the medium through a two-boson exchange and there is a resulting energy-momentum transfer rate. We will take the case of a fast quark propagating through a QGP (with the massless quark/antiquark component only) as an example to illustrate the details of the calculation and the resulting collisional energy loss. The setup is shown diagrammatically in Fig. 3, where the fast parton is represented by the blue fermion line. In Fig. 3 we focus on the contribution from $F^{\tau\lambda}(P_4, P_5)$ in Eq. (13). It includes an initial fast particle with momentum P, which interacts with the

medium and scatters into final state P_f. We find it contributes

$$F^{\tau\lambda}(P_4,P_5) = -2\pi i g^2 \int \frac{d^4P' d^3\mathbf{P}_f}{P_f} \times \frac{P^\tau P'^\lambda + P'^\tau P^\lambda - g^{\tau\lambda} P\cdot P'}{P'^2 + i\epsilon} \times [\delta^4(P - P_4 - P')\delta^4(P' - P_5 - P_f) + P_4 \leftrightarrow P_5]. \quad (37)$$

Combining Eq. (37) with Eq. (13) gives

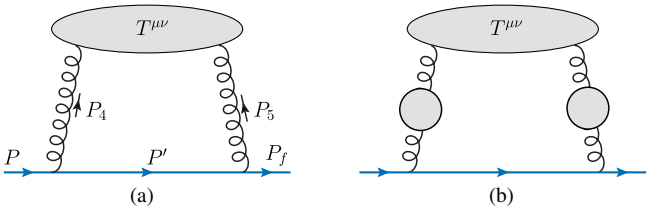

FIG. 3 (color online). Feynman diagrams for the source term in QCD in the presence of a fast parton with momentum P, which is represented by the blue fermion line. The diagram (a) is at tree level and contributes to the hard region. The diagram in (b) contributes to the soft region with the hard thermal loop; the resummed gluon propagator is indicated by a gray blob.

$$\partial_\mu T^{\mu\nu}(X) = -8ig^4 N_f C_2 \int \frac{d^4P_i}{(2\pi)^{11}} e^{-iX\cdot(P_4+P_5)} T(P_3) D_{\sigma\tau}(P_4) D_{\omega\lambda}(P_5) G_A(P_3 - P_4) \times [2(P_3{}^\sigma P_3{}^\omega - P_3{}^\sigma P_4{}^\omega)P_5^\nu + g^{\sigma\omega} P_3\cdot P_4 P_5^\nu - g^{\nu\sigma} P_3{}^\omega (2P_3\cdot P_5 - P_4\cdot P_5)] \times \int \frac{d^4P' d^3\mathbf{P}_f}{P_f} \frac{P^\tau P'^\lambda + P'^\tau P^\lambda - g^{\tau\lambda} P\cdot P'}{P'^2 + i\epsilon} [\delta^4(P - P_4 - P')\delta^4(P' - P_5 - P_f) + P_4 \leftrightarrow P_5]. \quad (38)$$

Equation (38) is then inserted in Eq. (6) to yield the collisional energy loss expression

$$\frac{dE}{dt} = 8N_F C_2 g^4 \int \frac{d^4P_3 d^4P_4}{(2\pi)^7} G_A(P_3 - P_4) n_F(p_3)\delta(P_3^2) D_{\sigma\tau}(P_4) D_{\omega\lambda}(-P_4) \frac{1}{E} \times [2(P_3{}^\sigma P_3{}^\omega - P_3{}^\sigma P_4{}^\omega)(-P_4)^\nu + g^{\sigma\omega} P_3\cdot P_4 (-P_4)^\nu - g^{\nu\sigma} P_3{}^\omega (-2P_3\cdot P_4 + P_4^2)] \times \left[\frac{P^\tau (P - P_4)^\lambda + P^\lambda (P - P_4)^\tau + g^{\tau\lambda} P\cdot P_4}{(P - P_4)^2 + i\epsilon} + \frac{P^\tau (P + P_4)^\lambda + P^\lambda (P + P_4)^\tau - g^{\tau\lambda} P\cdot P_4}{(P + P_4)^2 + i\epsilon}\right]. \quad (39)$$

In the soft region, we use the effective thermal propagator for the exchanged gluon, which is the same as that for the photon in Eq. (23) when the thermal photon mass is replaced with the thermal gluon mass. Using the same techniques as in the calculation of the collisional energy loss in the external current approach from the last section, we integrate over the angle of $\mathbf{p}_3$. The contribution from the interference between the longitudinal and transverse parts leads to zero, and the contributions from the longitudinal and transverse part are

$$\left.\frac{dE}{dt}\right|_{LL} = 4N_F C_2 g^4 \int \frac{dp_3 dp_4 dE_4}{(2\pi)^3} n_F(p_3) |\Delta_L(P_4)|^2 \mathrm{sgn}(p_3 - p_4\omega) p_3 E_4^2, \quad (40)$$

$$\left.\frac{dE}{dt}\right|_{TT} = 2N_F C_2 g^4 \int \frac{dp_3 dp_4 dE_4}{(2\pi)^3} n_F(p_3) |\Delta_T(P_4)|^2 \mathrm{sgn}(p_3 - p_4\omega) p_3 E_4^2 \left(1 - \frac{E_4^2}{p_4^2}\right)^2. \quad (41)$$

The complete result in the soft region is the sum of the longitudinal and transverse parts and we enforce an upper limit cutoff q^* of $\int dp_4$. We find that the result matches the one from the previous subsection in the limit of $u \to 1$ up to an additional color factor and the number of quark flavors:

$$\left.\frac{dE}{dt}\right|_{\mathrm{soft}} = \frac{N_F C_2 g^4 T^2}{24\pi} \int_0^{q^*} dp_4 \int_{-p_4}^{p_4} dE_4 E_4^2 \left[|\Delta_L(P_4)|^2 + \frac{1}{2}\left(1 - \frac{E_4^2}{p_4^2}\right)^2 |\Delta_T(P_4)|^2\right]. \quad (42)$$

In the hard region, we use the tree-level Feynman diagrams while ignoring any screening due to the plasma. The calculation is tedious but straightforward and yields

$$\left.\frac{dE}{dt}\right|_{\rm hard} = -2N_F C_2 g^4 \int \frac{dp_3 dp_4 dP_4^0 d\omega d\nu}{(2\pi)^3} p_3 p_4^2 n_F(p_3) \left[\frac{1}{(p_4^0)^2 - p_4^2}\right]^2 \frac{p_4^0}{\sqrt{p_3^2 + p_4^2 - 2p_3 p_4 \omega}}$$
$$\times \{[2p_3^2 E(2 + (1-\omega^2) + \nu^2(3\omega^2 - 1) - 4\nu\omega) - 4p_3 E(1 - \omega\nu)(p_4^0 - p_4\nu) - ((p_4^0)^2 - p_4^2)(p_4^0 - p_4 u)]$$
$$\times \delta(p_4^0(p_3 + E) - p_3 p_4 \omega - E p_4 \nu) + [2p_3^2 E(2 + (1-\omega^2) + \nu^2(3\omega^2 - 1) - 4\nu\omega)$$
$$- 4p_3 E(1 - \omega\nu)(p_4^0 - p_4\nu) + ((p_4^0)^2 - p_4^2)(p_4^0 - p_4 u)] \times \delta(p_4^0(p_3 - E) - p_3 p_4 \omega + E p_4 \nu)\}. \quad (43)$$

In the limit of $E \gg T \gg gT$, the integrals can be performed analytically

$$\left.\frac{dE}{dt}\right|_{\rm hard} = \frac{N_F C_2 g^4 T^2}{48\pi}\left[\ln\frac{q_m T}{(q^*)^2} + \frac{8}{3} - 12\ln(A) + \ln(4\pi)\right]. \quad (44)$$

Upon adding the hard and soft components the dependence on the separation scale q^* cancels and the total collisional energy loss is

$$\frac{dE}{dt} = \frac{N_F C_2 g^4 T^2}{48\pi}\left[\ln\frac{E}{g^2 T} + 2.725\right]. \quad (45)$$

One can immediately see that the collisional energy loss derived from the diagrammatic approach matches the one obtained from the external current approach.

IV. NUMERICAL RESULT

In this section, we present the result for the collisional energy and momentum loss of a fast lepton in an EPP and of a fast quark in the QGP, respectively. For direct comparison, just like in the earlier sections, we only consider scattering of the external parton with the quark-antiquark component of the QGP.

In principle, in the case of strong interactions the method to match the hard and soft momentum exchange contributions by introducing the arbitrary intermediate momentum scale $gT \ll q^* \ll T$ is only valid in the weak coupling limit $g \ll 1$. Here, we extend the numerical evaluation to moderate values of g for the purpose to investigating the dependence of collisional energy loss on the coupling constant g. The collisional energy loss as a function of the heavy quark energy E and coupling g is shown in Fig. 4, where a constant temperature $T = 250$ MeV and $N_F = 3$ have been chosen as typical for many phenomenological applications. In the left figure, the upper and lower surfaces are for charm quarks and bottom quarks, respectively. One can see that, for both charm and bottom quarks, the magnitude of collisional energy loss in QGP increases monotonically with initial energy E and coupling g. By comparing the collisional energy loss for charm and bottom quarks, one clearly sees the large mass effect that goes $\sim \ln(E/M)$ in Eq. (36) [$\ln(1/\sqrt{1-u^2}) = \ln(E/M)$]. The energy loss of a bottom quark is approximately half of the energy loss of charm quarks for $E \sim 10$–15 GeV. Note that one should not confuse the logarithmic growth of the collisional energy loss with larger jet quenching at higher energies E. It is the fractional energy loss $\Delta E/E$ that enters phenomenological applications [57,58] and it goes $\sim \ln(E/M)/E$. It is straightforward to extend our result

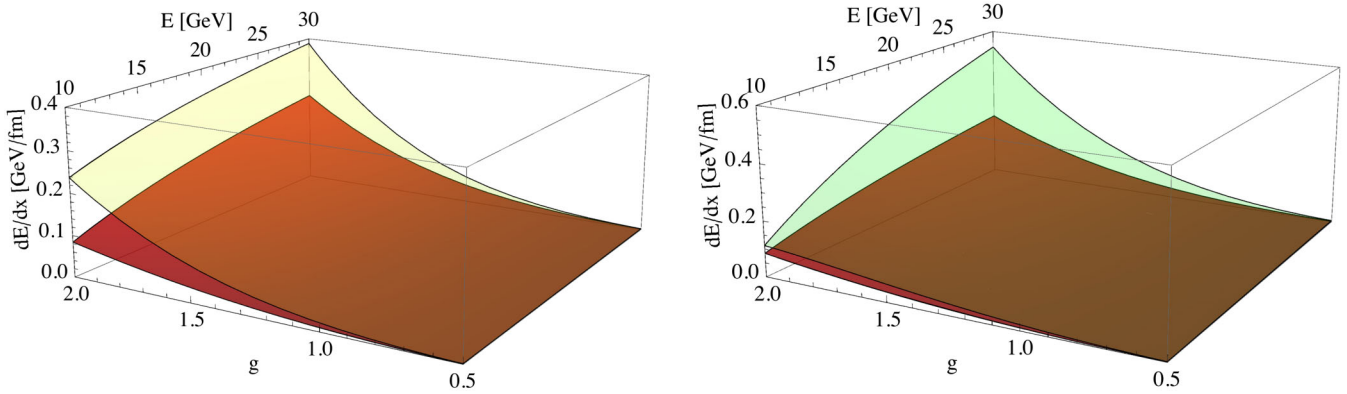

FIG. 4 (color online). A three-dimensional representation of collisional energy loss for heavy quarks versus energy E and coupling g. The left figure is the comparison of the energy loss rate of charm (yellow surface) and bottom (red surface) when the medium contains only the quark-antiquark component. The right figure is the bottom quark energy loss when the medium contains a quark-antiquark component only (red surface), and both quark-antiquark and gluon components (green surface). We have chosen $M_c = 1.5$ GeV and $M_b = 4.5$ GeV, respectively, a constant temperature $T = 250$ MeV and $N_F = 3$ as typical for many phenomenological applications of heavy-ion collisions.

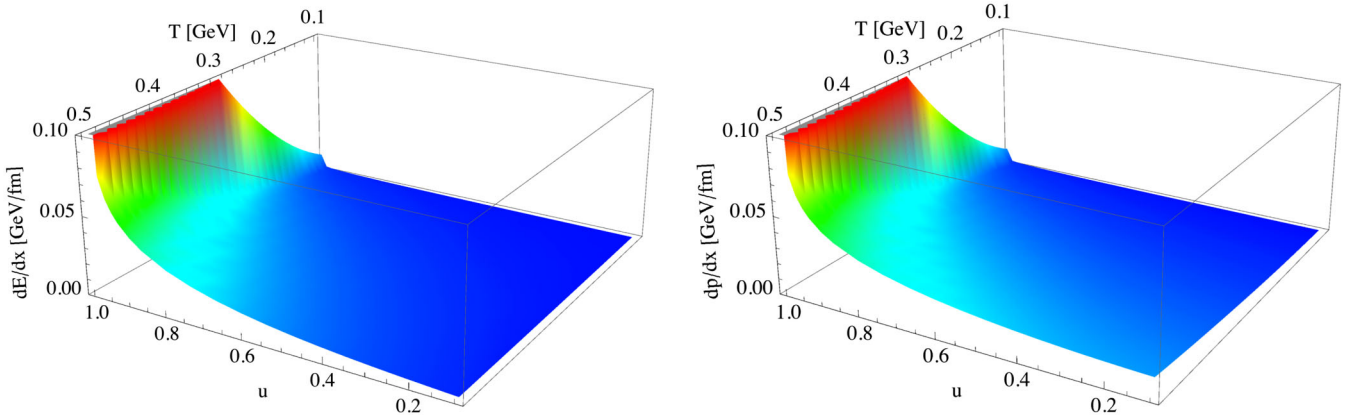

FIG. 5 (color online). Three-dimensional representations of collisional energy loss (left) and momentum loss (right) versus the temperature T and velocity u. A fixed coupling $g = 1$ has been chosen for the numerical evaluation. One can see that the momentum loss is larger than the energy loss in the small and moderate velocity regions.

from a quark-antiquark plasma to a quark-gluon plasma. The result should be the same as that from the scattering rate approach up to a minus sign, where the energy loss due to the gluon component is a factor of $6/N_F$ different from the one due to the quark-antiquark component to the leading logarithmic accuracy [27]. To compare these two results, we also plot in Fig. 4 the bottom quark collisional energy loss in quark-antiquark plasma (lower surface) and quark-gluon plasma (upper surface).

We also show in Fig. 5 the collisional energy loss (left panel) and momentum loss (right panel), where a fixed coupling $g = 1$ has been chosen. One can see that the collisional momentum loss behaves similarly to the energy loss; both of them increase monotonically with the temperature T and velocity u. In the small and moderate velocity regimes, the momentum loss is larger than the energy loss, due to the finite velocity effect, as one can see from Eq. (32). We mention here that in the ultrarelativistic limit

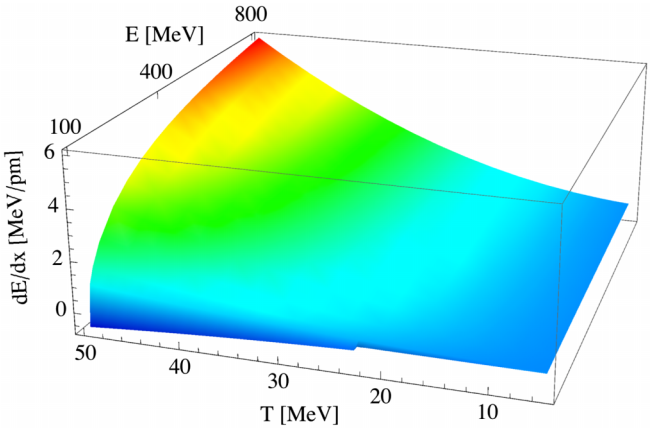

FIG. 6 (color online). A three-dimensional representation of the collisional energy loss versus the energy E and temperature T for a heavy muon propagating through an EPP. The muon mass is $M_\mu = 105$ MeV; the elementary charge is fixed at $e = 0.3$ (in terms of natural units), corresponding to a fine structure constant $\alpha = 1/137$.

$u \to 1$ and nonrelativistic limit $u \to 0$, the formula Eq. (36) for collisional energy loss that we have used for the numerical evaluation of Fig. 5 breaks down. Therefore, physical kinematics should be imposed to compute the collisional energy as we presented in the last section.

Next, we extend the numerical examples to the case of relativistic QED plasmas that can be produced in high-intensity laser fields and play a role in various astrophysical situations, such as in supernova explosions. We show in Fig. 6 an example of the collisional energy loss from temperatures $T = 10$–50 MeV that can be typically realized in laser produced and supernova electron-position plasmas [59]. In the relativistic plasma we considered here, $T \gg m_e$, so that the mass of the electron and positron in the medium can be neglected. The elementary charge $e = 0.3$, corresponding to a fine structure constant $\alpha = 1/137$, indicates that one can distinguish the soft and hard momentum scales, i.e. $eT \ll T$, and the EPP is weakly coupled. Therefore, the result we derived in this paper should give a good description of the physics. Shown in Fig. 6 is the collisional energy loss in QED as functions of the initial muon energy E and medium temperature T. The collisional energy loss increases with the increasing of the medium temperature; for example, this leads to an energy loss of 3 MeV/pm for a muon with energy $E = 200$ MeV at $T = 50$ MeV.

V. SUMMARY

In this paper we considered energetic charged particle propagation in an EPP and a QGP (quark-quark scattering only). We derived the energy and momentum absorbed by the medium per unit time when the particle is slowed down due to collisional interactions. For this purpose, starting from the medium's point of view, we provided an operator definition of collisional energy and momentum transfer rate based upon the divergence of the medium EMT. By using an external current approach, we evaluated the energy and

momentum loss of an energetic lepton passing through a thermal electron-positron plasma. Furthermore, in a more general diagrammatic approach we considered the collisional energy loss of a fast parton in the QGP. In both cases we applied the method used by BT to separate the exchanged momenta into hard and soft regions, to evaluate the relevant HTL resummed and tree-level diagrams. We showed explicitly that the newly developed formalism leads to results which are infrared safe, independent of gauge and any separation scales. Our results for the energy-momentum absorption rate by the medium reproduce (up to the anticipated minus sign) the well-known results for the energy loss of an energetic charged particle from the scattering rate approach. To illustrate the analytic results, we gave examples of an energetic heavy quark propagating through the quark-gluon plasma, which can be produced in heavy-ion collisions, and an energetic muon traveling in electron-positron plasma, which can be produced in high-intensity laser fields. In summary, we found that up to the expected difference in the energy, temperature, coupling strength and degrees of freedom, the collisional energy-momentum transfer rates in QED and QCD behave very similarly. It will be instructive in the future to carry out such a comparison beyond the weakly coupled regime using numerical techniques.

ACKNOWLEDGMENTS

This work was supported in part by the U.S. Department of Energy, Office of Science.

[1] M. Gyulassy, I. Vitev, X.-N. Wang, and B.-W. Zhang, in *Quark Gluon Plasma 3*, edited by R. C. Hwa and X.-N. Wang (World Scientific, Singapore, 2003), pp. 123–191.
[2] R. B. Neufeld, I. Vitev, and B.-W. Zhang, Phys. Lett. B **704**, 590 (2011).
[3] H. Xing, Y. Guo, E. Wang, and X.-N. Wang, Nucl. Phys. **A879**, 77 (2012).
[4] M. Gyulassy and X.-N. Wang, Nucl. Phys. **B420**, 583 (1994).
[5] R. Baier, Y. L. Dokshitzer, A. H. Mueller, S. Peigne, and D. Schiff, Nucl. Phys. **B484**, 265 (1997).
[6] M. Gyulassy, P. Levai, and I. Vitev, Nucl. Phys. **B594**, 371 (2001).
[7] B. G. Zakharov, JETP Lett. **65**, 615 (1997).
[8] X.-N. Wang and X.-f. Guo, Nucl. Phys. **A696**, 788 (2001).
[9] P. B. Arnold, G. D. Moore, and L. G. Yaffe, J. High Energy Phys. 06 (2002) 030.
[10] S. S. Adler *et al.* (PHENIX Collaboration), Phys. Rev. Lett. **96**, 032301 (2006).
[11] A. Adare *et al.* (PHENIX Collaboration), Phys. Rev. Lett. **98**, 172301 (2007).
[12] M. M. Aggarwal *et al.* (STAR Collaboration), Phys. Rev. Lett. **105**, 202301 (2010).
[13] B. Abelev *et al.* (ALICE Collaboration), J. High Energy Phys. 09 (2012) 112.
[14] B. Abelev *et al.* (ALICE Collaboration), Phys. Rev. Lett. **109**, 112301 (2012).
[15] H. van Hees and R. Rapp, Phys. Rev. C **71**, 034907 (2005).
[16] S. Wicks, W. Horowitz, M. Djordjevic, and M. Gyulassy, Nucl. Phys. **A784**, 426 (2007).
[17] P. B. Gossiaux and J. Aichelin, Phys. Rev. C **78**, 014904 (2008).
[18] R. Sharma, I. Vitev, and B.-W. Zhang, Phys. Rev. C **80**, 054902 (2009).
[19] J. Uphoff, O. Fochler, Z. Xu, and C. Greiner, Phys. Lett. B **717**, 430 (2012).
[20] T. Renk, Phys. Rev. C **80**, 044904 (2009).
[21] Y. He, I. Vitev, and B.-W. Zhang, Phys. Lett. B **713**, 224 (2012).
[22] R. B. Neufeld and I. Vitev, Phys. Rev. Lett. **108**, 242001 (2012).
[23] C. E. Coleman-Smith and B. Muller, Phys. Rev. C **86**, 054901 (2012).
[24] W. Dai, I. Vitev, and B.-W. Zhang, Phys. Rev. Lett. **110**, 142001 (2013).
[25] J. Huang, Z.-B. Kang, and I. Vitev, Phys. Lett. B **726**, 251 (2013).
[26] J. D. Bjorken, Report No. FERMILAB-PUB-82-059-THY, 1982.
[27] E. Braaten and M. H. Thoma, Phys. Rev. D **44**, 1298 (1991); **44**R2625 (1991).
[28] K.-I. Nishikawa, P. Hardee, G. Richardson, R. Preece, H. Sol, and G. J. Fishman, Astrophys. J. **622**, 927 (2005).
[29] S. Mrowczynski and M. H. Thoma, Annu. Rev. Nucl. Part. Sci. **57**, 61 (2007).
[30] F. Wang, Prog. Part. Nucl. Phys. **74**, 35 (2014), and references therein.
[31] Michael E. Peskin and Dan V. Schroeder, *An Introduction to Quantum Field Theory*, Frontiers in Physics (Westview Press, 1995).
[32] J. D. Jackson, *Classical Electrodynamics* (John Wiley and Sons, New York, 1998), 3rd ed.
[33] R. B. Neufeld and B. Muller, Phys. Rev. Lett. **103**, 042301 (2009).
[34] G.-Y. Qin, A. Majumder, H. Song, and U. Heinz, Phys. Rev. Lett. **103**, 152303 (2009).
[35] H. Li, F. Liu, G.-l. Ma, X.-N. Wang, and Y. Zhu, Phys. Rev. Lett. **106**, 012301 (2011).
[36] H. Stoecker, Nucl. Phys. **A750**, 121 (2005).
[37] J. Casalderrey-Solana, E. V. Shuryak, and D. Teaney, J. Phys. Conf. Ser. **27**, 22 (2005); Nucl. Phys. **A774**, 577 (2006).
[38] R. B. Neufeld and T. Renk, Phys. Rev. C **82**, 044903 (2010).

[39] A. K. Chaudhuri and U. Heinz, Phys. Rev. Lett. **97**, 062301 (2006).
[40] B. Betz, J. Noronha, G. Torrieri, M. Gyulassy, and D. H. Rischke, Phys. Rev. Lett. **105**, 222301 (2010).
[41] S. S. Gubser, S. S. Pufu, and A. Yarom, Phys. Rev. Lett. **100**, 012301 (2008).
[42] P. M. Chesler and L. G. Yaffe, Phys. Rev. D **78**, 045013 (2008).
[43] J. Noronha, M. Gyulassy, and G. Torrieri, Phys. Rev. Lett. **102**, 102301 (2009).
[44] I. Bouras, A. El, O. Fochler, H. Niemi, Z. Xu, and C. Greiner, Phys. Lett. B **710**, 641 (2012).
[45] P. Chakraborty, M. G. Mustafa, and M. H. Thoma, Phys. Rev. D **74**, 094002 (2006).
[46] J. J. Friess, S. S. Gubser, G. Michalogiorgakis, and S. S. Pufu, Phys. Rev. D **75**, 106003 (2007).
[47] A. Yarom, Phys. Rev. D **75**, 105023 (2007).
[48] P. M. Chesler and L. G. Yaffe, Phys. Rev. Lett. **99**, 152001 (2007).
[49] R. B. Neufeld, Phys. Rev. D **83**, 065012 (2011).
[50] R. B. Neufeld and I. Vitev, Phys. Rev. C **86**, 024905 (2012).
[51] T. Kashiwa and N. Tanimura, Fortschr. Phys. **45**, 381 (1997).
[52] A. K. Das, *Finite temperature field theory* (World Scientific, Singapore, 1997), p. 404.
[53] E. Braaten and R. D. Pisarski, Phys. Rev. Lett. **64**, 1338 (1990); Nucl. Phys. **B337**, 569 (1990); **B339**310 (1990).
[54] E. Braaten and T. C. Yuan, Phys. Rev. Lett. **66**, 2183 (1991).
[55] G. Ovanesyan and I. Vitev, J. High Energy Phys. 06 (2011) 080.
[56] R. B. Neufeld, Phys. Rev. D **78**, 085015 (2008).
[57] I. Vitev, Phys. Lett. B **639**, 38 (2006).
[58] Z.-B. Kang, I. Vitev, and H. Xing, Phys. Lett. B **718**, 482 (2012).
[59] M. H. Thoma, Rev. Mod. Phys. **81**, 959 (2009).